Talanta 223 (2021) 121617

Contents lists available at ScienceDirect

Talanta

journal homepage: www.elsevier.com/locate/talanta

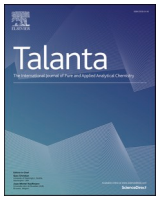

Robust and sensitive peptidomics workflow for plasma based on specific extraction, lipid removal, capillary LC setup and multinozzle ESI emitter

Bertrand Rochat [a,b,*], Patrice Waridel [a], Jachen Barblan [a], Pierre-Edouard Sottas [c], Manfredo Quadroni [a]

[a] Protein Analysis Facility, University of Lausanne, Switzerland
[b] University Hospital of Lausanne, 1015, Lausanne, Switzerland
[c] Chem. des Uttins 4, 1028, Préverenges, Switzerland

ARTICLE INFO

Keywords:
Blood
High-resolution mass spectrometry
Plasma
Peptide
Multi-nozzle electrospray
Statherin

ABSTRACT

We present a new workflow for the LC-MS determination of native peptides in plasma at picomolar levels. Collected whole blood was quickly diluted with an ice-cold solution in order to stop protease activity. Diluted plasma samples were extracted by protein denaturation followed by solid-phase-extraction with a polymeric stationary phase that removed most proteins and lipids. Using a specific LC-MS setup with 3 pumps, 240 μL of extracts were injected without drying-reconstitution, a step known to cause peptide losses. After an 18-fold dilution on-line, peptides were trapped on a 1 × 10 mm C8 column, back-flushed and resolved on a 0.3 × 100 mm C18 column. Extract reproducibility, robustness (column clogging), extraction yields, matrix effects, calibration curves and limits of detection were evaluated with plasma extracts and spiked-in standards. The sensitivity and applicability of 3 electrospray sources were evaluated at capillary flow rates (10 μL/min). We show that ionization sources must have a spray angle with the MS orifice when "real" extracts are injected and that a multinozzle emitter can improve very significantly peptide detection. Finally, using our workflow, we have performed a peptidomics study on dried-blood-spots collected over 65 h in a healthy volunteer and discovered 5 fragments (2.9–3.8 KDa) of the protein statherin showing circadian oscillations. This is the first time that statherin is observed in blood where its role clearly deserves further investigations. Our peptidomic protocol shows low picomolar limits of detection and can be readily applied with or without minor modifications for most peptide determinations in various biomatrices.

1. Introduction

Natural peptides are widely recognized as key regulators in living systems [1–4]. As agonists or antagonist of various receptors and enzymes and cell membrane disruptors, they can act as hormones, local messengers, antibiotics, etc. Interestingly, many essential bioactive peptides have been identified only within these last 2 decades, e.g. ghrelin, hepcidin, kalata B1, odilorhabdin, hemopressin, SQS peptide [5–10]. Many others will probably be uncovered in mammals or plants thanks to technical or methodological advancements.

The determination of peptides needs discriminating detection such as mass spectrometry in order to reveal peptide length or mass, peptide sequence and post-translational modifications (PTM). Indeed, once the active peptides are produced from proteins and pro-peptides by enzymatic cleavage [1,3] or from direct mRNA translation of short-open-reading-frames (sORF) [12], their fate in plasma or tissues is controlled by the activity of many proteases/peptidases [11,13]. In addition, modifications of peptide structure (e.g. PTM such as amidation, acetylation, methylation, phosphorylation etc or cleavage of one terminal amino acid) can have significant consequences on peptide biological activity.

Immunoassays have been the standard methodology for the sensitive detection of peptides in biomatrices and should still play a major role in cost-effective and high-throughput analyses (e.g. cardiac troponin I, a small protein of 23 KDa, or the 3.5 KDa brain natriuretic peptide) [14,15].

However, the main weaknesses of antibody-based assays (that-is-to-say the cross-reactivity with various molecular species) are amplified

* Corresponding author. Protein Analysis Facility, University of Lausanne, Switzerland.
E-mail addresses: bertrand.rochat@chuv.ch (B. Rochat), patrice.waridel@unil.ch (P. Waridel), jachen.barblan@unil.ch (J. Barblan), pesottas@gmail.com (P.-E. Sottas), manfredo.quadroni@unil.ch (M. Quadroni).

https://doi.org/10.1016/j.talanta.2020.121617
Received 16 June 2020; Received in revised form 31 August 2020; Accepted 1 September 2020
Available online 8 September 2020

with small amino acid chain (<50) and low MW (<5 KDa) in comparison with bigger proteins [16,17]. Even if mass spectrometry is often less sensitive then immunoassays, it still appears as the technology of choice to discover and study the fate of peptides with unambiguous identification.

Whereas we know the importance of many peptides in living organisms, the peptidome (defined as all peptides in a living organism), was described as a *terra incognita* in 2005 [1]. Nevertheless, peptidomics is a very promising field for new discoveries, in which LC-MS plays a central role [18]. For this reason, since a decade or two, a significant effort has been done to study the peptidome, even if specific publications still represents only 1% of the total in the proteomics field (see Fig. 1S in Supplementary Material). Numerous LC-MS methods for peptide determination have been published [19–23]. Their sample preparations are mainly protein precipitation, solid phase extraction, tryptic digestion, decoupled LC fractionation, ultra-filtration and immuno-extraction. The LC-MS part uses triple-quadrupole or high-resolution MS instruments in a classical 1D-LC or preconcentration LC setups with trap and analytical columns whose inner diameters (i.d.) range from 2.1 (macrobore) to 0.075 mm (nano). Last but not least, various dedicated peptidomics softwares were recently developed to help the identification of large undigested peptides.

Nevertheless, today it still remains challenging to develop a peptidomics LC-MS analysis method for small to large (5–50 AA length), hydrophilic to hydrophobic and amphiphilic peptides at picomolar levels, i.e. the concentrations at which these peptides are found *in vivo*, in plasma or other biomatrices. Indeed, many peptidomics methods use different steps that are known to be very disadvantageous to the determination of long and hydrophobic peptides, such as poor sample stabilization during the very first step of biomatrix withdrawal or a drying-reconstitution step.

In this article, we describe the development of a peptidomics workflow using LC-high resolution (HR)-MS, which significantly improves on our previous method [24] in both analytical robustness and sensitivity. The biomatrix used for this development was human plasma but the workflow could be adapted to other biomatrices, such as urine, saliva, tissue homogenate etc. The sample cleanup of our previous protocol [24] was a protein precipitation with acetonitrile (MeCN) followed by ultrafiltration. This did not remove sufficiently debris and phospholipids (Fig. 2S) that rapidly accumulated in the LC-system [25] and consequently reduced the robustness of this previous assay (short column life time and rapid overpressure with <100 sample extracts). Building on our previous experience, we have systematically evaluated and modified several steps in the workflow to address numerous issues.

In summary, the described generic peptidomics workflow couples SPE extraction with direct injection of undried extracts on a specific LC-MS platform (Fig. 1) with a multinozzle electrospray (ESI) emitter that improves peptide detection at capillary flow rates (10 μL/min). We believe that only minor modifications would be needed for adapting this workflow to specific peptide chemistries and different matrices.

As a proof of concept, we have applied this workflow and LC-HRMS platform in a preliminary peptidomics study. We have determined peptides in dried blood spots collected over 65 h in a healthy volunteer and, for the first time, identified 5 truncated peptides of the protein statherin which undergo circadian oscillations.

2. Material and methods

2.1. Chemicals and materials

Formic acid (FA), heptafluorobutyric acid (HFBA), urea, guanidinium hydrochloride (Guan) and protease-inhibitor-cocktail (PIC) were purchased from *Sigma-Aldrich* (Buchs, Switzerland) *or Thermo Fisher Scientific* (Waltham, MA USA). Organic solvents such as acetonitrile (MeCN) were Lichrosolve-grade and purchased from Merck. Pure standard peptides were obtained from in-house tryptic digestion of pure bovine BSA standard, *Thermo Fisher Scientific*, *Bachem* (Basle, Switzerland), *Phoenix Europe* (Karlsruhe, Germany) or were a kind gift of Prof. Oleg Krokhin (University of Manitoba, Winnipeg, Canada) (Fig. 2S). Peptide stock solutions were prepared in water:MeOH, 70:30 (v/v) at high concentration (>100 μM). Injection tubes, Eppendorfs, 96 well plates, falcon tubes and tips were all in polypropylene. Blood collection tubes were *Vacuette K2EDTA* (K2E 3 mL) from *Greiner Bio-One*, although other tubes were also tested (see Section 3.1.1.). For solid-phase-extraction and lipid removal, please see Section 2.3.2.

2.2. LC-MS system and conditions

The LC setup is described in Fig. 1 and is based on a *Thermo* Ultimate 3000 module. It is composed of an autosampler (*Thermo* WPS-3000TFC), maintained at 5°C, with a 250 μL injection loop and a column oven set at 60°C, two 10-port valves, a binary pump (P1; *Thermo* micro LPG NCS-3500RS) used to load the sample, an additional quaternary pump (P2, *Thermo* LPG-3400SD) used to dilute on-line the loaded sample prior the trap column and a capillary pump (P3, *Thermo* cap NCS-3500RS). The *Ultimate* module has a flow-selector (ProFlow™) for 5–50 μL/min flow rates. The enrichment step was done on a 1 × 10 mm, 3.5 μm Hypersil Gold C8 column (*Thermo Fisher Scientific*) and the chromatography was performed on various C18 analytical columns with 200 or 300 μm (i.d.), 50 or 150 mm length, 2.7–3.5 μm particle size and 160 to 300 Å pore size (Zorbax 300Extend-C column from *Agilent Technologies*, Santa Clara, CA, USA or MonoCap C18 Fast-Flow column from *GL Sciences*, Tokyo, Japan or Ascentis Express Peptide ES-C18 from *Supelco, Darmstadt, Germany*). A filter with 0.5 μm porosity was placed between the autosampler and the trap column and was cleaned by a back-flush flow (Fig. 1). Mobile phases were A: 0.1% (v/v) FA for P1 and P3 or 0.1% HFBA for P3 in water and B: MeCN with 0.1% FA (v/v) for all pumps. Typical pump flow rates, valve positions and gradient elution are given in Fig. 1. At t = 0 min, the flow rates were 55, 950 and 10 μL/min for P1, P2 and P3, respectively. The trapping time was 5 min. Analytes were back-flushed to the C18 analytical column. During analyte elution, P1 and P2 flow rates were reduced to 10 and 50 μL/min, resp. Mass calibration was done with mobile phase contaminants (polysiloxane and diisooctyl phthalate at *m/z* at 445.1206 and 391.2848, respectively) at the beginning of each run between 3.5 and 4 min. Total run time varied from 20 to 60 min, depending on column length and purpose of analysis.

The LC system was coupled with a Q-Exactive Plus HRMS (*Thermo Fisher Scientific*) working with an electrospray source (ESI) in positive mode. The following 3 ESI sources (Fig. 3S) were tested at 10 μL/min with pure standards in solvent or in plasma extracts: 1) the HESI-II probe (*Thermo Fisher Scientific*) set with a micro-needle (50 μM inner diameter) dedicated for low flow rate, 2) an EASY-Spray transfer line (*Thermo Fisher Scientific*) with a 20 μM inner diameter silica emitter and 3) a M3 multinozzle emitter (*NewOmics*, Berkeley, CA, USA). MS full scan and Data-Dependent-Acquisition (alternating a full scan and product ion scans) were performed in profile mode. Additional MS parameters (mass resolution, spray voltage, collision-induced-dissociation value, source N_2 flow, etc) were depending on the experiments and are given in the *Results*.

2.3. Blood withdrawal and plasma cleanup

2.3.1. Whole blood withdrawal and plasma preparation

Whole blood (WB) samples were withdrawn by venipuncture from healthy volunteers in 3 mL K2E *Vacuette* tubes and under local ethical agreement rules. In order to stop the degradation of peptides as quickly as possible, 2 protocols were tested: 1) the addition of protease-inhibitor-cocktail (PIC) in the collection tubes and 2) based on a previous report [31], the dilution of WB with an isotonic ice-cold 0.9% NaCl solution immediately after its collection. The second protocol was preferred (see *Results*) and is described below. Immediately after WB collection, the blood tube was inverted 2× and opened. Immediately, 1

volume of WB (e.g. 0.6 ml) was transferred in a 2 mL Eppendorf tube containing 1 vol (0.6 mL) of an ice-cold 0.9% NaCl isotonic solution. The entire operation takes less than 0.75 min. The Eppendorf tube was placed on crushed ice for 2–10 min (not more than 60 min) and centrifuged at 1800 g at 4°C for 10 min. The supernatant, corresponding to 2.9× diluted plasma (mean dilution value), was transferred in polypropylene tube(s) and kept at 4°C for direct extraction or at −20°C for > 24 h storage.

The dilution of whole blood with a cold solution adds a small inaccuracy in the quantitative analysis of peptides and metabolites in plasma. Indeed, the plasma dilution factor depends on the hematocrit. Hematocrit is defined as the ratio of the volume of red blood cells to the total volume of blood. In humans, normal women and men hematocrits fluctuate between 0.36 and 0.48 and 0.40 and 0.54, respectively. When considering a 2× WB dilution and using the average hematocrit values for men and women, 0.47 and 0.41, the bias to quantify peptides and metabolites in a 2× diluted whole blood is less than 10% and plasma is diluted 2.9× ± 9.9% and 2.7× ± 8.5% for a men and women, respectively (refer to Table 1S for calculation). When the hematocrit of men or women living at high altitude is considered, this bias increases to a maximum of 25% (Table 1S). In this case, adapted hematocrit values could be used or an internal standard could be added to the dilution solution.

2.3.2. Plasma extraction

Our goal here was to improve our previous sample cleanup [24] by removing more extensively the debris and phospholipids. Various protocols were tested, e.g. protein precipitation with MeCN in combination with different lipid-removal well-plates such as Captiva™ (*Agilent*) and Phree™ (*Phenomenex*) or the Supel™ Genie HybridSPE® (*Supelco*) On-line SPE Cartridges. Lipid removal is based on the capture of 1) the phospho-head group by ZrO_2 or TiO_2 phases or 2) the long aliphatic chains by stationary phases showing size exclusion and strong hydrophobic interactions. Finally, SPE with Oasis® HLB_{PRiME} 96 well plates (*Waters*, Milford, MA, USA; 10 mg of stationary phase) was tested and adopted (see the *Results*). A potential drying-reconstitution step was also evaluated for peptide losses. Spiked (known) and native (unknown) peptides were used to test the extraction protocols. Ions with a charge state ≥2, symmetric peak shapes and appropriate isotopic distributions were considered as native peptides.

Here below, we describe the chosen peptide extraction workflow with its 2 main steps. Step 1 was the pretreatment of the diluted plasma (obtained from diluted WB; see 2.3.1.). One volume of diluted plasma samples (typically 0.9 mL) was mixed with 1 volume of a solution of 3 M Guanidine hydrochloride (Guan) and 3 M Urea in water. These 2 chaotropic agents were added to unfold proteins and peptides, to break protein-protein and peptide-protein interactions and to stop protease activities.

The mixture was vortexed for 60 min at 4°C. Step 2 was SPE on a 96 well-plate containing 10 mg of HLB_{PRiME} phase: for each step, the plate was centrifuged at 250g for 5 min at room temperature (*Eppendorf* centrifuge 5804 with A-2 DWP rotor). Diluted plasma samples (0.9 mL, corresponding to 300 µl of blood) pretreated with the chaotropic agents (0.9 mL), were directly loaded in the wells (1.8 mL) containing 100 µL of 10% FA (final 0.5% FA); the washing step was done with 1.0 mL of 1% FA:MeOH, 95:5 (v/v). Peptides were eluted in the injection plate with 280 µL of MeCN:MeOH 90:10 (v/v), which were diluted by adding 320 µL of H_2O in the well prior to the last centrifugation. Organic content in the final eluates is ≈ 50% for a total volume of 600 µl.

2.4. Validation of the peptidomics workflow

2.4.1. Peptide trapping

Peptide trapping with large injection volumes (up to 750 µL) containing 50% MeCN by on-line dilution has been previously described [24]. Similar trapping was re-evaluated with the new sample cleanup but smaller injection volumes (250 µL). Peak area reproducibility of peptides injected as pure standards or in extracts, both solutions containing 50% MeCN, was determined in relationship to the on-line dilution factor (10–20 fold).

2.4.2. Matrix effect, extraction yield, limits of detection and robustness of the protocol

We have evaluated our protocol from the point of view of extraction yields, matrix effects, limits of detection of various peptides, robustness (defined as LC system overpressure/clogging) and analytical reproducibility. Prior to extraction, some plasma samples, called *SB* for *spiked before*, were spiked with various levels (from 28 to 700 pM) of peptides not found in human plasma. The list of the spiked peptides is given in Fig. 2S. Post-extraction, some plasma extracts, called *SA* for *spiked after*, were spiked with the same peptides at the same levels. Finally, *NO* samples, for no-matrix-no-extraction, were prepared by adding the same peptides at the same levels in MeCN, MeOH, 1% FA in water and DMSO at 20:10:65:5, respectively (v/v/v/v). All sample types were analyzed in the same LC-HRMS sequence. Extracted-ion-chromatograms (XIC) of spiked peptides were constructed and their peak area was determined. *SB/SA* and *SA/NO* peak area ratios for each peptide were calculated to determine the extraction yields and matrix effects, respectively. The limits of detection were determined with calibration curves where the peptides were spiked in 250 µL of plasma at the following levels: 0, 1, 2.5, 5, 10, 25, 50, 100, 250, 500, 1000 and 2500 pM, and extracted. The limit of detection (LOD) was found with the most intense ion and was defined when the peak area was obtained with ≥7 MS unsmoothed scans, a S/N ≥ 7, an area value ≥ 5× the blank plasma extract and an accuracy ≤ ±30% (calculated with the calibration curve equation). Evaluation of the method robustness was based on the increase of pressure on C8 and C18 columns and deterioration of chromatography. Contaminants and debris (e.g. lipids, proteins, polyethylene glycol, etc) in our sample extracts were surveyed.

2.4.3. Evaluation of the performance of 3 types of ESI sources

Since a few years, various companies have developed ESI source dedicated to capillary flows (5–50 µL/min) to fill the gap between nano-ESI and ESI sources designed for of 0.2–1 and 100–800 µL/min flow rates, respectively. For instance, *Waters*, *Sciex* (Framingham, MA, USA) *and Thermo Fisher Scientific* have developed the IonKey/MS™, Opti-Flow™ and EASY-Spray™ ion sources designed for capillary flows. LC-ESI-MS detection is often considered as concentration-dependent, whereby the sensitivity theoretically increases as the column inner diameter squared ratio. This means that, at similar amounts on column, a 0.3 mm i.d. column should show a 49× sensitivity improvement in comparison to a 2.1 mm i.d. column $[(2.1)^2/(0.3)^2]$. A complementary view is to consider that the sensitivity depends on the molecule concentration *in the gas phase of the ionization source*. In this case, at similar amounts on column, the improvement of sensitivity will depend on the concentration in the mobile phase, the compound peak width and the ionization yield. In this second scenario, the ionization source efficiency is clearly significant.

Thus, we have tested the performance of the 3 following ESI sources at 10 µL/min flow rate: 1) a classical ESI, the *Thermo* HESI-II, with a microneedle dedicated to capillary flow, 2) the EASY-Spray™ and 3) the *Newomics* M3 multinozzle emitter with its disposable 8 nozzle device (Fig. 3S). For this evaluation, pure peptide standards in solvent and plasma extracts were injected on our LC-HRMS setup.

2.5. Use of the peptidomics workflow

Our workflow was tested in a preliminary peptidomics study with the aim to uncover peptides with circadian oscillations. Dried blood spots (DBS) were collected regularly over 65 h in a healthy volunteer with Hemaspot™-SE devices (San Francisco, CA, USA, SpotOnScience.com; see Fig. 4S). Thirteen blood collections were done as follows: Day 1:

10h00, 12h30, 16h00, 19h30, 23h15, 03h00, 04h30; Day 2: 07h00, 10h30, 11h50, 3h00; Day 3: 03h00.

The Hemaspot™-SE device allows separating blood cells and serum from a finger prick. Three blood drops (≈60–90 μL) were collected on the device. Blood cells (mainly erythrocytes), remain concentrated in the center of the paper (red part) that is cut in a spiral form, while serum migrates to the end of the spiral arm (orange part), away from the blood cells. Two and three 6 mm diameter punches of blood containing cells and serum, respectively, of the same collection paper were put in two distinct Eppendorf tubes for extraction. Each punch corresponds on average to 8 μL of serum or blood cells. For the reconstitution of the dried blood cells and serum, 400 μL of 3 M Guan and urea denaturating solution were added in each Eppendorfs containing the paper punches. Reconstituted samples were then treated according to our workflow and analyzed with our LC-HRMS platform using the *NewOmics* M3 multi-nozzle ESI emitter. First, a LC-HRMS analysis with full scan acquisition from *m/z* 350 to 1200 was performed for circadian peptide discovery. A second analysis with Data-Dependent-Acquisition that combines full scan and product-ion-scan (MS^2) acquisitions was performed for peptide sequence identification (see the *Results* for details). Progenesis QI software (version 2.3; NonlinearDynamics, Newcastle upon Tyne, UK) was used for identifying, through label-free quantitation, peptides showing concentrations with circadian oscillations. Peak area were normalized using the default Progenesis normalization, based on total metabolites abundance (a weighting factor based on intensity of all detected features). In order to remove false positive peptides, data were treated with stringent parameters removing peaks with poor chromatographic peak shapes, small differences between day and night levels, very low peak area, inconsistent isotopic distributions and non-circadian profiles. Revealed circadian peptides were putatively identified by MS^2 spectra with *PEAKS Studio* software (see the *Results* for details).

3. Results and discussion

The new workflow is presented and is based on the following central choices that we have made: 1) ultra-rapid whole blood (WB) stabilization by immediate dilution with ice-cold NaCl solution, temperature drop and protease activity inhibition, 2) protein denaturation prior the extraction to free all endogenous peptides from protein binding, 3) solid-phase-extraction (SPE) that removes most protein and lipid content to avoid strong matrix effects and their accumulation in the LC system, 4) the absence of a drying-reconstitution step to avoid peptide losses [19,21,26–30], 5) the possibility to inject large volumes (up to 250 μL) with high organic content (SPE eluate from the previous step) thanks to an on-line dilution allowing peptide refocusing on a trap column, 6) the resolution of peptides on a capillary analytical column (0.3 mm i.d.) as the best compromise between sensitivity and robustness 7) improved peptide detection by a multinozzle ESI emitter and 8) the selective detection of peptides by high-resolution mass spectrometry (HRMS) employing MS^1 and MS^2 acquisition modes. Reverse phase C8 and C18 columns were used in this work as they represent by far the most used chromatography in peptide analysis. However, other stationary phases could be used like polystyrene-divinylbenzene, hydrophilic interaction liquid chromatography (HILIC) when more specific peptide chemistries (hydrophilic peptides) or problems (strong peptide adsorption) will have to be addressed.

3.1. Blood withdrawal and plasma cleanup

3.1.1. Whole blood withdrawal and plasma preparation

First, we evaluated the risk to add contaminants in our samples from blood collection tubes. We found that Sarstedt K-EDTA S-monometer tubes released large amounts of polyethylene glycol in contrast to *Vacutainer* and *Vacuette* K2EDTA tubes that were preferred.

Protease-inhibitor-cocktails (PIC), commercially available in DMSO solution or from tablets to dissolve in water, allow inhibiting a large spectrum of protease activities. PIC are usually composed of AEBSF, aprotinin, bestatin, E64, eupeptic, pepstatin A and EDTA that are added in the blood sample at the following final concentrations, 1,000, 0.8, 50, 15, 20, 10 and 5,000 μM, respectively. At final recommended concentrations in whole blood, PIC add 1% DMSO in blood that lyses blood cells and prevent its use in blood collection tubes. Preparations of PIC as tablets contain detergents to ensure proper solubility and these are then released in solution. Detergents are known to perturb chromatography and ionization. Small detergent amounts may have minor effects on macrobore column (2.1 mm i.d.) and ionization process at high flow rates ≥ 100 μL/min. But if concentrated on capillary columns (≤0.5 mm i.d.), they can cause real analytical problems. As depicted in Fig. 5S, Triton, a well known detergent, was introduced in our sample from a PIC solution prepared from tablets. Consequently, many massive and broad chromatographic peaks of Triton were observed (Fig. 5S) in plasma extracts, resulting in a peptide ion suppression and decrease of MS sensitivity.

For this reason, an alternative to PIC was investigated in order to inhibit protease activities during the sample withdrawal. Whole blood (WB) dilution with a cold solution, immediately after collection, was tested according to a previous report [31] with minor modifications. WB withdrawal procedure and dilution is realized in ≤45 s and is described in Section 2.3.1. As it is shown in Fig. 2C, when a 2× dilution is done, the blood temperature immediately drops to 12.5°C and when the blood tube is further placed on crushed ice, the temperature drops to 10°C in ≤0.5 min and is below 5°C after 2 min. With a 3× dilution, the temperatures drops more rapidly but the difference with a 2× dilution was considered as minor. Thus, for our protocol, we have chosen a 2× dilution as the best compromise between sample dilution and inhibition of protease activities by cold temperatures. After 2–10 min, the tubes containing the 2× diluted WB were centrifuged and diluted plasma (2.9× ± 10%; see 2.3.1) was transferred to new tubes for direct extraction or storage at −20°C.

According to our experiments (see below) and previously published work, protease activities are reduced to < 10% at 10°C and <5% at 5°C in various living systems [32–34]. The “exceptions” are bacteria found in Antarctica/Artica sea water where proteases activity can still be significant at 10°C (20% of maximum activity) [35]. Nevertheless, a very quick drop of temperature to 5°C after sample withdrawal, appears as a cheap and convenient solution to efficiently inhibit protease activities (see Section 3.2.2). This protocol of blood collection and dilution is appropriate for peptidomic studies whereas slightly less feasible in hospitals. However, usual procedure of blood withdrawal in hospitals (blood tubes at room temperature for 1–3 h prior centrifugation and cooling) can be sufficient if the peptide to be determined is stable enough in blood (long half-life).

3.1.2. Plasma extraction

In order to improve the sample cleanup of our previous work [24], different lipid removal steps were tested off-line with Captiva™, Phree™ and HLB_{PRiME} 96-well plates or on-line with the Supel™ Genie HybridSPE® Cartridges. The Genie HybridSPE® retained too strongly our test peptides and LC conditions needed to obtain peptide elution did elute lipids as well. In contrast, Captiva™, Phree™ and HLB_{PRiME} well-plates removed the majority of phospholipids such as phosphocholine species that were detected by the marker fragment ion at *m/z* 184.07332 ($[C_5H_{15}O_4NP]^+$) generated by in-source decay (Fig. 3) [25]. Little differences in peptide extraction characteristics were observed (Table 1). The main problem is that the protocols used with Captiva™ and Phree™ plates request to dilute 3 to 5 times the sample with MeCN. This eventually demands to dry and reconstitute the large eluate volumes in order to reduce both volumes and percentage of solvent before injection on reverse phase LC columns. But it is known that a drying step results often in strong peptide losses (adsorption or aggregations) [19,21,26–29]. In our sample extracts, strong peptide losses (especially with ≥2.5 KDa peptides) were observed after drying

Table 1
Detection of endogenous plasma peptides in LC-HRMS analyses after 5 different extractions.

MW (kDa)		1–10	1–4	4–10
# of peptides		N = 152	N = 98	N = 54
# of peptides (N)				
PP-S [a]	2	100	100	100
PP-UF [b]	4	95	129	37
HLB prime [c]	12	57	68	38

Values are ratios (in %), calculated from LC-MS peak-area relatively to the values found in the protein precipitation supernatant (PP–S; [a]). Observed multicharged ions ($z \geq 2$ with appropriate isotopic distributions, see Methods section) were considered as peptides. [a]: Plasma extracted by protein precipitation with 1 volume of MeCN. [b]: Plasma extracted by protein precipitation with 1 volume of MeCN followed by ultrafiltration of the supernatant with a MWCO = 30 kDa (see [23] for additional details). [c] Plasma extracted by 3 different solid-phase extractions in 96 well-plates.

(Fig. 6S).

Eventually, we choose to use the polymer-based HLB_{PRiME} phase (see complete protocol in *Material and methods* section). The lack of silanol groups, the capability to remove salts, proteins and lipids more efficiently (Fig. 3) and the elution with small volumes (25–250 µL for 2–10 mg of SPE phase that are compatible with direct injections on our specific LC setup after reduction of MeCN content to 50%) were the HLB_{PRiME} main advantages for our protocol.

3.2. Validation of the peptidomics workflow

3.2.1. Peptide trapping

Peak area reproducibility (coefficient of variation, CV) was evaluated with ≥5 replicate injections (250 µL) of 5 peptides in pure solvent or in plasma extracts (both at 50% organic content). Good reproducibility was more difficult to obtain with extracts. However, CV improved from 55% ± 24 to ≤12% ± 11 when the dilution factor during peptide trapping, increased from 10× to ≥15×. Therefore, we modified our previous loading step from 10× [24] to 18× on-line dilution with loading and dilution pumps at 55 and 950 µL/min, respectively (Fig. 1). Fig. 7S shows the pump pressures during the analysis.

3.2.2. Robustness, matrix effects, extraction yield, limits of detection and robustness of the protocol

LC robustness was evaluated by the increase in backpressure on columns and deterioration of chromatographic quality after injections of SPE extracts. We observed an increase of pressure on the filter and trap column (Fig. 8S) necessitating replacing the filter and/or the trap column regularly (after approx. 100 samples injected). This fouling effect was clearly the results of remaining proteins from the extract precipitating or aggregating (Fig. 8S). Therefore, we tested a new LC configuration using two 10-port valves, in which the filter is cleaned after each injection by back-flushing it with mobile phase (Fig. 1 or 9S, for the comparison between the classical 2 columns setup and our setup). This clearly improved the uptime before an irreversible increase of pressure is observed on the column (Fig. 8S).

Matrix effects and extraction yield were calculated from peak area ratios of peptides spiked in matrix prior or after extraction vs. in pure solvent (see Section 2.4.2). Results are depicted as overall means in

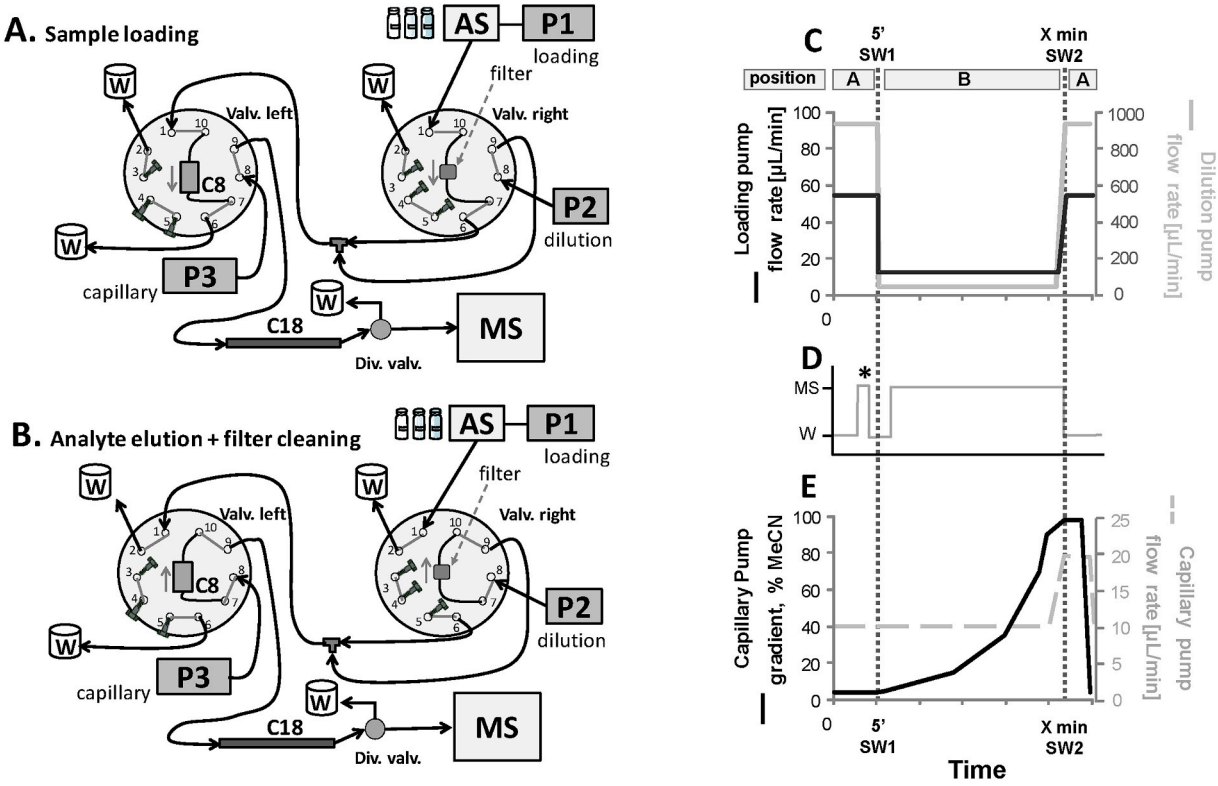

Fig. 1. Scheme of the LC setup for the new workflow. Position **A**: the sample is loaded on the trap column; Position **B**: trapped analytes are back-flushed and resolved whereas the filter is cleaned. **C**: flow rate of the pump loading the sample (P1) and of the pump diluting the sample on-line (P2). For loading, P1 and P2 deliver 100% of 0.1% FA. P1 and P2 pump flows decrease to very low rates when both valves are switched to position **B** and mobile phases switch to 0.1% FA in MeCN. **D**: the divert valve allows the mobile phase to go to the MS or the waste; (*) mobile phase of P3 is diverted to MS for mass calibration. **E**: flow rate of the capillary pump (P3) and gradient elution are depicted. ***Abbreviations***: AS: autosampler; C8: 1 × 10 mm i.d. X L column; C18: 0.2/0.3 × 50–150 mm i.d. X L column; MeCN: acetonitrile, SW: Switch time for A and B positions; W: waste; X min: adaptable gradient time. See *Supplementary Figure 9S* for pump pressure profiles.

Table 2
Quantitative evaluation of the new peptidomics workflow.

	Matrix effetcs [%] (N = 28)	Extraction Yield [%] (N = 23)	LOD* [pM] (N = 11)
Mean values	103	118	54
minima	37	34	2.5
maxima	210	179	250

Matrix Effect (%), Extraction Yield (%) and Limits of Detection (pM) of 28, 23 and 11 synthetic spiked-in peptides, respectively, for 250 μL of plasma extracted (or 725 μL of plasma when prepared from 2× diluted whole blood). Limits of detection (*LOD) were evaluated taken into account a S/N ratio ≥ 5; ≥7 scans and ≥ 5× blank peak area.

Table 2 or in more details in Fig. 10S. The overall means indicate low matrix effects and good extraction yields. Distribution of individual values (Fig. 10S) and minimum and maximum values (Table 2) reveal relatively large variability. Matrix effects with values that are >100% probably reflect protective effects of the matrix against peptide adsorption on surfaces, whereas extraction yields that are >100% suggest that there was a slight difference between the real spiked levels in the matrix before and after the extraction, again as a probable consequence of peptide adsorption. Nevertheless, the distributions of the matrix effects and extraction yields (for 28 and 23 peptides, respectively) indicate that this is a suitable generic plasma cleanup for peptidomics analysis.

Limits of detection (LOD) were established with calibration curves of 11 spiked-in peptides extracted from 250 μl of undiluted plasma corresponding to 725 μl of diluted plasma when prepared from a 2× diluted whole blood (see Section 2.3.1). Examples of calibration curves are depicted in Fig. 10S. Mean LOD value is 54 pM. The lowest LOD value is 2.5 pM and obtained for a BSA tryptic fragment, BSA480 (chromatograms and curve in Fig. 10S). The mean LOD, 54 pM, is 4× lower than with our previous method [24] obtained with 3× more plasma volume and using an LTQ ion trap MS (*Thermo*) where mean LOD obtained with 9 other peptides was 217 pM. While the overall gain shows roughly a 12× improvement, the LOD still appears too high for many *in vivo* peptide levels in human plasma. Thus, to increase sensitivity, alternative ESI sources were tested (see 3.2.3).

Next we assessed the capacity and saturation limits of 10 mg of HLB_{PRiME} phase, by loading 100, 250, 350, 500, 750 and 1000 μL of undiluted plasma. As depicted in Fig. 11S, a maximum of 500 μL of plasma (corresponding to ≈ 30–40 mg of proteins) can be loaded in our conditions before a clear loss of proportionality of response is observed.

Finally, the stability of blood and plasma matrices at 4°C was studied by recording peptides that were found to increase with time when tubes were left at room temperature. Fig. 2 depicts i) the time course of 8 endogenous peptides produced in whole blood (WB) at 4 and 37°C, ii) the time course of 10 peptides produced in plasma at 4 and 37°C and iii) the time course of 3 peptides produced/released at 4°C in whole blood immediately cooled by dilution. The data shows that, according to the recorded peptides, ice-cold temperatures inhibit proteases activity and stabilize plasma and whole blood for a few hours. In WB at 4°C (Fig. 2D), no peptide increased dramatically in the first hour, and only 3 peptides eventually increased over longer times (>2h). This indicates that the immediate temperature drop by WB dilution with an ice-cold isotonic solution (Fig. 2C; see 2.3.1.) and the WB centrifugation within an hour, is an effective protocol to stabilize blood and prepare plasma.

3.2.3. *Evaluation of the performance of 3 types of ESI sources*

The performance of 1) HESI-II, 2) EASY-Spray and 3) M3 multinozzle emitter (see designs on Fig. 3S), were tested at a flow rates of 10 μL/min. First, we observed that the spray alignment had a great impact on robustness. Indeed, when the spray was directly aligned to the MS entrance (ions and neutrals following a straight line), the entrance of the mass spectrometer was rapidly obstructed (Fig. 12S). This was observed with the EASY-Spray source when our plasma extracts were injected. In contrast, when the spray direction shows a significant angle with the MS entrance, e.g. M3 multinozzle emitter or the classical HESI-II source, such clogging was not observed before the injection of >100 of samples (Fig. 12S). This is in agreement with the off-axis design of other capillary flow ESI sources Optiflow™ and Ionkey/MS™. Classical nano-source designs show sprays that are aligned with the MS entrance. This is compatible with the extremely clean samples typically injected in proteomic analysis. However, usual sample preparations from biofluids in routine analysis (e.g. SPE) produce extracts that still contain some amounts of lipids and intact proteins (Fig. 8S). In this case, off-axis sprays appear mandatory. For this reason, the EASY-spray source was abandoned despite showing a 4–5x sensitivity improvement in comparison to HESI-II (data not shown).

Fig. 4 shows the gain of sensitivity obtained using the M3 multinozzle emitter vs. the HESI-II source, measured on 10 peptides in plasma extracts and over a 3 days of analysis. The average gain is 24.4× with a minimum of 6× and a maximum of 60×. The sensitivity gain correlates positively with the charge state, *z* (Fig. 4), but does not correlate with the retention times. The M3 emitter also shows a better spray stability and peak width (−36%) than HESI-II as it is representatively depicted with hepcidin, a 2.8 kDa endogenous peptide (Fig. 13S; sensitivity gain between 11 and 37× depending on *z*). For all the above reasons, we used the M3 multinozzle emitter in the preliminary circadian peptidomics study (below).

3.3. *Use of the peptidomics workflow*

As a proof of concept, we applied the new workflow for a preliminary study of the circadian evolution of the plasma peptidome in a healthy volunteer. Samples were conveniently collected as dried blood-spots using the Hemaspot™-SE system. Fig. 5A depicts a peptide, P3821 ($z = 4$), showing a circadian variation, revealed after data treatment with Progenesis QI software. Extracted-ion-chromatograms and isotopic distribution of P3821 are depicted in Fig. 5B. Using "stringent" treatment of this first LC-HRMS data acquisition (performed in full scan acquisition only), no other peptides were identified as circadian.

A second LC-HRMS analysis was performed with data-dependent-acquisition (MS^2 spectra) for peptide identification. Fig. 5C depicts the sequence identified by *PEAKS Studio* software (ID score, $-10lgP = 69.8$; mass accuracy = 1.2 ppm; more details are given in Fig. 14S). P3821 is a 32 amino acid length peptide which is a truncated form of human statherin protein spanning residues 30–61 (STATH: UniProtKB - P02808; see https://www.uniprot.org/). STATH 20–62 is a 43 amino acid protein that is active after the loss of the signal peptide (1−19). *PEAKS Studio* software identified other truncated forms of STATH 20–62 protein in our analysis. We reprocessed the first data acquired and performed relative quantification of the newly discovered truncated forms. Four STATH additional peptides showed circadian oscillations in blood (Fig. 15S). These peptidic fragments are in the C-terminal region of STATH: STATH 30–61 (P3821), 33–61 (P3495), 33–62 (P3642), 30–56 (P3138) and 40–62 (P2901) (Fig. 15S). The mean peak area ratios between samples taken during the night or the day, are between 3.5 and 21 fold (*P-values* ≤ 0.05; Fig. 15S). This indicates that the levels of these 5 peptides are significantly more abundant in blood during the night.

We validated the identification of the STATH peptides by analyzing an extract of saliva, a fluid in which the protein is known to be abundant in humans [36,37]. STATH 20–62 and the 5 truncated forms discovered in blood, STATH 30–61, 33–61, 33–62, 30–56 and 40–62 were detected in saliva, with matching *m/z* values and relative RT values (Fig. 16S). However, to the best of our knowledge, this is the first time that STATH 30–61, 33–61, 33–62, 30–56 and 40–62 peptides are detected in blood collected in dried blood spots (Fig. 15S). The STATH peptides found in dried blood spots were also detected in plasma (diluted whole blood protocol) in parallel to the detection of hepcidin, a peptidic hormone

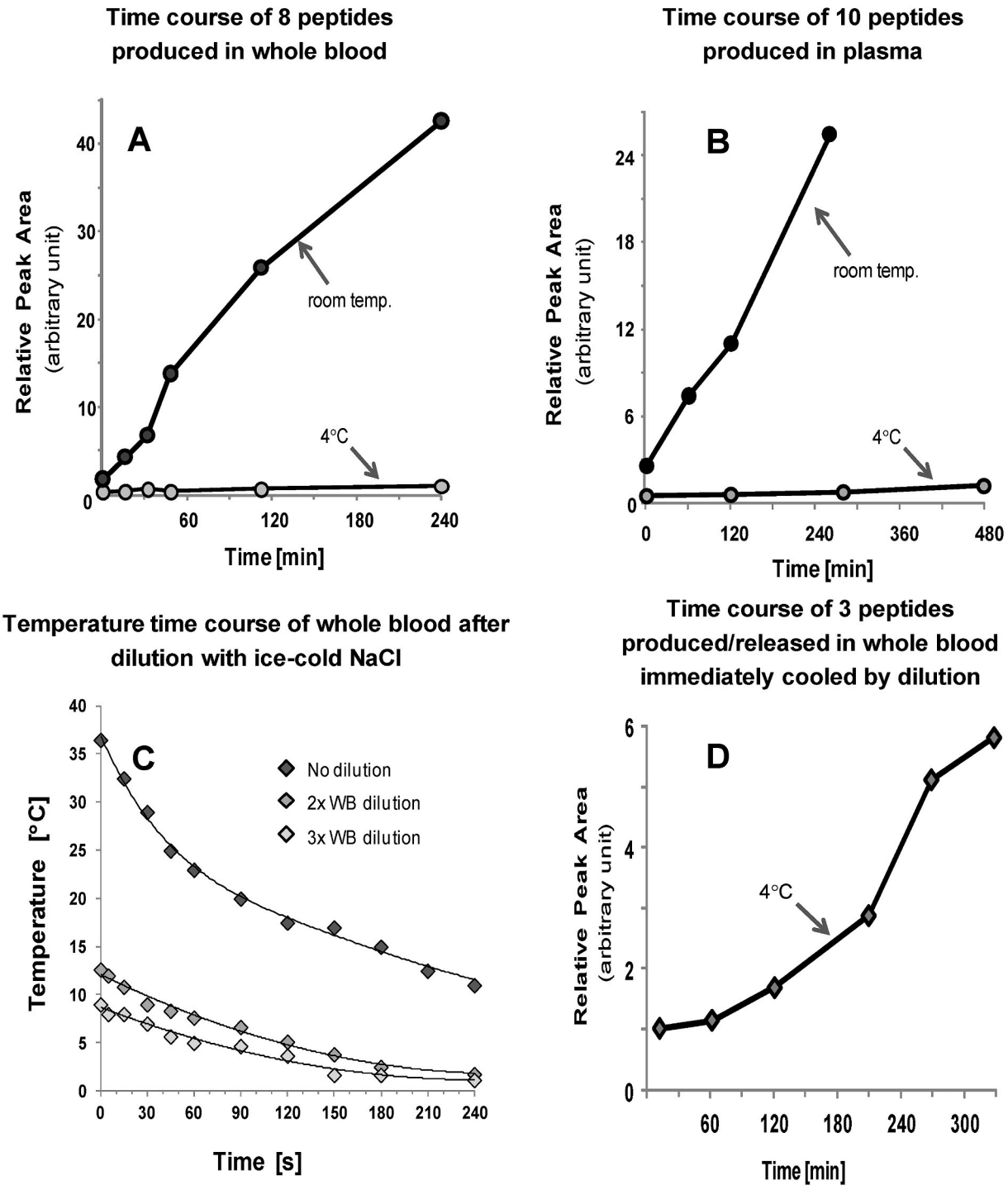

Fig. 2. **A**. Time course of 8 peptides in undiluted whole blood (WB) at 4°C or room temperature (21°C). **B.** Time course of 10 peptide in plasma at 4°C or RT°. **C.** WB temperature time course (in sec.). After WB withdrawal, 1 mL was quickly transferred in a tube containing an ice-cold NaCl solution and put on crushed ice. After dilution, temperatures drop immediately at $\leq$ 12.5°C, $\leq$ 10°C in $\leq$ 0.5 min and $\leq$ 5°C in 2 min **D.** Time course of 3 peptides in WB prepared by quick 2x ice-cold dilution. In A, B and D, relative peak area means of peptides are depicted. In **A**, **B** and **D**, all depicted peptides are different and endogenous.

found in blood but not in saliva. Therefore, it becomes of interest to understand what could be the role of STATH peptides in blood and why they show a circadian rhythm.

STATH (20–62) is a 43 amino acid long peptide that shows various functions in the oral cavity: it regulates tooth biomineralization via hydroxyapatite ($Ca_5(PO_4)_3(OH)$), protects enamel through formation of the acquired enamel pellicle (a protein bacteria-free biofilm). STATH also inhibits the growth of calcium phosphate minerals like dental calculus (tartar), increases calcium phosphate solubility, binds specific bacteria species fimbriae (e.g. *P. gingivalis*) and controls oral microbiota, aggregates bacteria and shows antibiotic activity [36–42]. The N-terminus (20–28 or 20–34) of STATH shows one or two phosphorylated serines and is associated with the binding to hydroxyapatite whereas the C-terminus is associated with the interaction with bacteria.

According to 2 online databases (biogps.org and proteomicsdb.org), in human tissues STATH gene expression (Fig. 17S) is high mainly in salivary glands but also in trachea, thalamus, thyroid and prostate. At the protein level, STATH tryptic peptides were found in blood platelets,

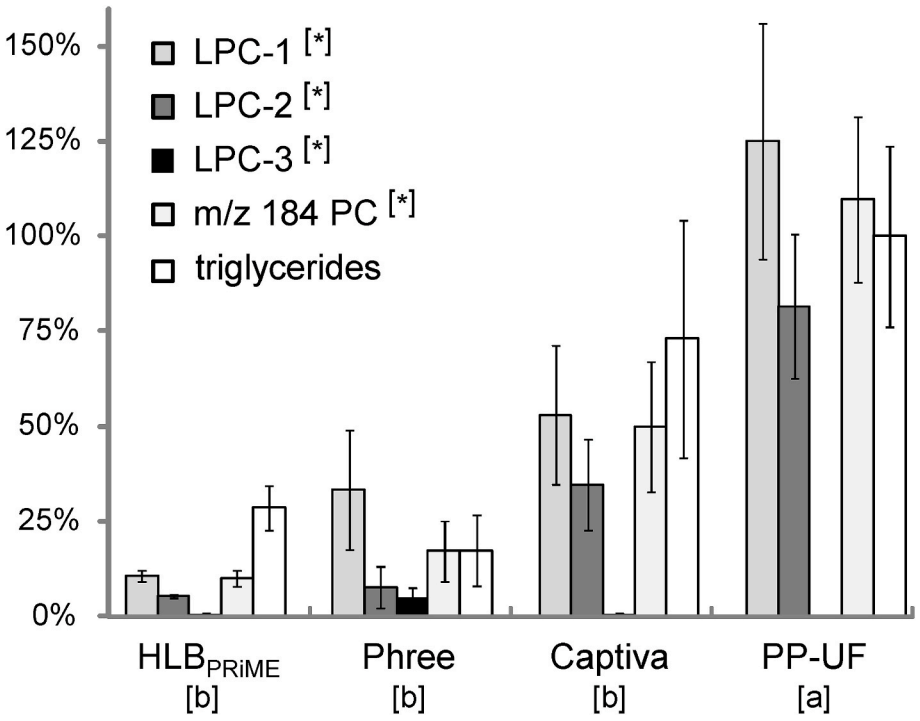

Fig. 3. Lipids detected in LC-HRMS analyses after plasma extractions with SPE plates or protein precipitation followed by ultrafiltration (PP-UF). Values are mean ratios (in %; N > 4), calculated from LC-MS peak-area relatively to peak area found in plasma supernatants after protein precipitation alone. **[*]** Lipids detected by LC-HRMS; LPC-1 to −3: 3 lysophospholipid species; PC: phosphatidylcholine species detected by the marker ion at *m/z* 184.07332 ([C5H15O4NP]+) [24]. **[a]**: Plasma extracted by protein precipitation with 1 volume of MeCN followed by ultrafiltration of the supernatant with a MWCO = 30kDa. **[b]**: Plasma extracted by 3 different solid-phase extractions in 96 well-plates.

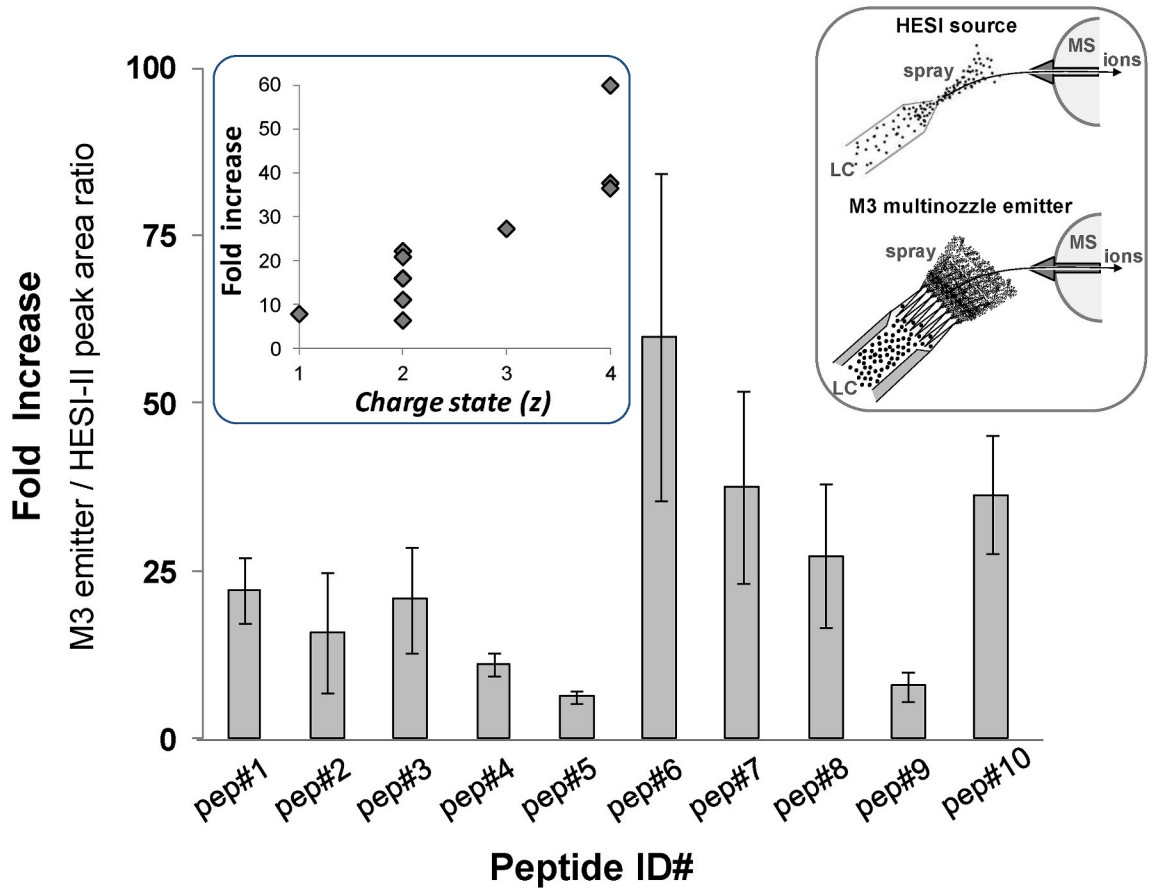

Fig. 4. Side-by-side comparison of peptide detection with 2 types of sources: a classical ESI source, HESI-II, and a multinozzle ESI emitter (M3 emitter, *Newomics*). Results, given as fold increase, are expressed as M3 emitter/HESI-II peak area ratio of peptides detected by LC-HRMS in plasma extracts. Shown is the mean ± SD of 10 determinations performed over a period of 10 days. Left-hand-side insert: fold increase related to peptide charge state (*z*). Right-hand-side insert: schematics of ion sources.

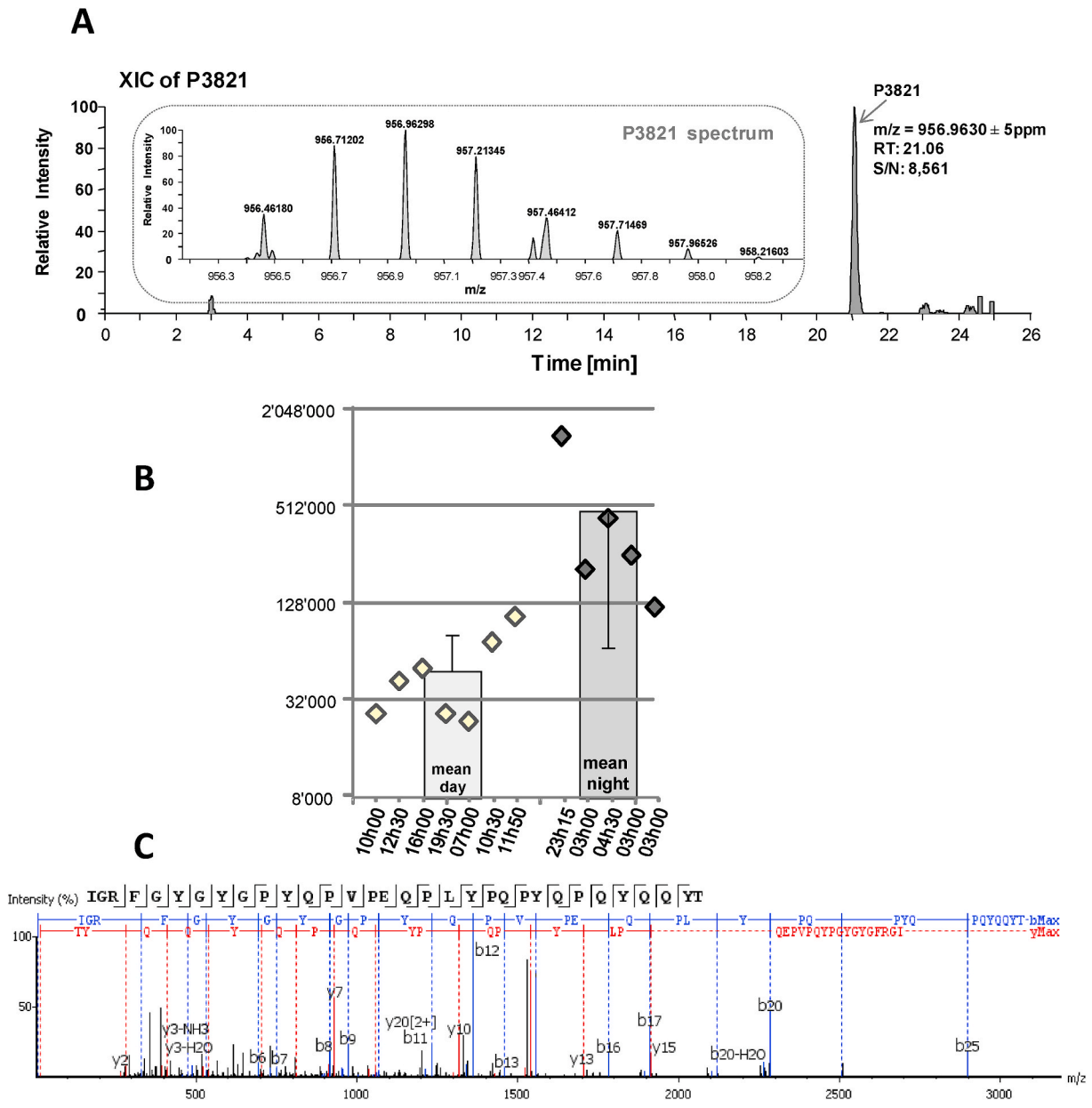

Fig. 5. A. Extracted-ion-chromatogram (XIC) is depicted for P3821 (*m/z* at 956.96298; A+2 isotope) with, in the insert, its isotopic distribution. **B.** Peptide ion P3821 (*m/z*monoisotopic at 956.46180; $z = 4$) was found to have higher levels in the night in dried serum spots collected from a healthy volunteer over a 65h circadian period (*P-value* ≤ 0.05) **C.** P3821 was identified as the 30–61 truncated form of human statherin, has 32 amino acids and its MWmonoisotopic is 3821.8154 Da.

urine and vitreous humor (Fig. 17S). Of note, thalamus, hypothalamus and the suprachiasmatic nucleus are considered as the primary circadian pacemakers [43,44]. Therefore, it can be hypothesized that the thalamus releases STATH peptide(s) according to a circadian clock.

The vascular role of STATH remains to be investigated but some hypotheses can be made based on STATH circadian oscillation, the main function of STATH (its binding to calcium phosphate) and some associations between published articles. When sleep duration is reduced or perturbed, there are increased risks of vascular calcification, atherosclerosis, endothelial microparticle production and osteoporosis [45–51]. Higher calcium levels in blood are also associated with atherosclerosis [51]. In addition, calcium levels in blood and vascular contractibility shows a circadian rhythm [52,53]. Thus, we could postulate that STATH circadian oscillation has a vascular role in relation with calcium, endothelial cells (blood vessels) and that this role is increased during the night. At the light of these results, further studies should be carried out.

4. Conclusion

By systematic redesign and optimization of a series of steps, we have significantly improved a previous peptidomics workflow for plasma or other biomatrices. Reproducibility and robustness were increased by stronger on-line dilution (≥15×), by removing lipids and other debris by SPE with a polymeric phase and by back-flushing an on-line filter between each sample. Sample preparation is rapid and dedicated to peptide determinations. After whole blood withdrawal, the quick dilution of the blood with ice-cold NaCl solution, protein denaturation before extraction, the absence of a drying-reconstitution step and large injection volume (250 µL) are key parameters of this peptidomics workflow. The use of 3 LC pumps, a trap and analytical columns (1 and 0.3 mm i.d.), an on-line filter that is cleaned between each sample and the use of a

multinozzle emitter constitute the originality of the LC-MS setup. With the M3 mulinozzle emitter, peptide detection was significantly improved and should allow quantification and discovery of many endogenous peptides at *in vivo* levels.

Novelty statement

Peptidomics protocol allowing robust and sensitive analysis with original LC set-up and an ESI source with multi-nozzle emitter. Application of the protocol allowing, for the first time, the discovery of fragments of the protein statherin in human blood showing circadian oscillations.

Author contribution

Bertrand Rochat, Conceptualization, method development, Formal analysis, Data curation, Writing and editing. Patrice Waridel, MS instrument maintenance and purchase, Supervision, Project administration, Writing - review & editing. Jachen Barblan. Pierre-Edouard Sottas, Conceptualization, method development, Formal analysis, Data curation, Writing and editing, Manfredo Quadroni, MS instrument maintenance and purchase, Supervision, Project administration, Writing - review & editing.

Declaration of competing interest

The authors declare that they have no known competing financial interests or personal relationships that could have appeared to influence the work reported in this paper.

Acknowledgements

The authors are grateful to Séverine Lorrain, Alexandra Potts-Xenarios and Lorenz Weidenaeur for their laboratory help or helpful discussion.

Appendix A. Supplementary data

Supplementary data to this article can be found online at https://doi.org/10.1016/j.talanta.2020.121617.

References

[1] P. Schulz-Knappe, M. Schrader, H.D. Zucht, The peptidomics concept, Comb. Chem. High Throughput Screen. 8 (2005) 697–704, https://doi.org/10.2174/138620705774962418.
[2] R. Vitorino, Digging deep into peptidomics applied to body fluids, Proteomics 18 (2018), https://doi.org/10.1002/pmic.201700401, 10.1002/pmic.201700401.
[3] K. Boonen, J.W. Creemers, L. Schoofs, Bioactive peptides, networks and systems biology, Bioessays 31 (2009) 300–314, https://doi.org/10.1002/bies.200800055.
[4] N. Farrokhi, J.P. Whitelegge, J.A. Brusslan, Plant peptides and peptidomics, Plant Biotechnol. J 6 (2008) 105–134, https://doi.org/10.1111/j.1467-7652.2007.00315.x.
[5] M. Kojima, H. Hosoda, Y. Date, M. Nakazato, H. Matsuo, K. Kangawa, Ghrelin is a growth-hormone-releasing acylated peptide from stomach, Nature 402 (1999) 656–660. https://doi:10.1038/45230.
[6] A. Krause, S. Neitz, H.J. Mägert, et al., LEAP-1, a novel highly disulfide-bonded human peptide, exhibits antimicrobial activity, FEBS Lett. 480 (2000) 147–150. https://doi:10.1016/s0014-5793(00)01920-7.
[7] O. Saether, D.J. Craik, I.D. Campbell, K. Sletten, J. Juul, D.G. Norman, Elucidation of the primary and three-dimensional structure of the uterotonic polypeptide kalata B1, Biochemistry 34 (1995) 4147–4158. https://doi:10.1021/bi00013a002.
[8] E. Racine, M. Gualtieri, From worms to drug candidate: the story of odilorhabdins, a new class of antimicrobial agents, Front. Microbiol. 10 (2019) 2893. https://doi:10.3389/fmicb.2019.02893.
[9] V. Rioli, F.C. Gozzo, A.S. Heimann, et al., Novel natural peptide substrates for endopeptidase 24.15, neurolysin, and angiotensin-converting enzyme, J. Biol. Chem. 278 (2003) 8547–8555. https://doi:10.1074/jbc.M212030200.
[10] Y. Takemoto, D. Mao, L.L. Punzalan, S. Götze, S.I. Sato, M. Uesugi, Discovery of a small-molecule-dependent photolytic peptide, J. Am. Chem. Soc. 142 (2020) 1142–1146. https://doi:10.1021/jacs.9b09178.
[11] B. Magalhães, F. Trindade, A.S. Barros, et al., Reviewing mechanistic peptidomics in body fluids focusing on proteases, Proteomics 18 (2018), e1800187. https://doi:10.1002/pmic.201800187.
[12] S.J. Andrews, J.A. Rothnagel, Emerging evidence for functional peptides encoded by short open reading frames, Nat. Rev. Genet. 15 (2014) 193–204. https://doi:10.1038/nrg3520A.
[13] V. Hook, L. Funkelstein, D. Lu, S. Bark, J. Wegrzyn, S. R Hwang, Proteases for processing proneuropeptides into peptide neurotransmitters and hormones, Annu. Rev. Pharmacol. Toxicol. 48 (2008) 393–423. https://doi:10.1146/annurev.pharmtox.48.113006.094812.
[14] C. Jungbauer, J. Hupf, E. Giannitsis, et al., Analytical and clinical validation of a point-of-care cardiac troponin T test with an improved detection limit, Clin. Lab. 63 (2017) 633–645. https://doi:10.7754/Clin.Lab.2016.160814.
[15] L.K. Lewis, S.D. Raudsepp, T.G. Yandle, T.C. Prickett, A.M. Richards, Development of a BNP1-32 immunoassay that does not cross-react with proBNP, Clin. Chem. 63 (2017) 1110–1117. https://doi:10.1373/clinchem.2016.269712.
[16] A.K. Saenger, O. Rodriguez-Fraga, R. Ler, et al., Specificity of B-type natriuretic peptide assays: cross-reactivity with different BNP, NT-proBNP, and proBNP peptides, Clin. Chem. 63 (2017) 351–358. https://doi:10.1373/clinchem.2016.263749.
[17] M. Ostrowska, Z. Bartoszewicz, T. Bednarczuk, K. Walczak, W. Zgliczyński, P. Glinicki, The effect of biotin interference on the results of blood hormone assays, Endokrynol. Pol. 70 (2019) 102–121. https://doi:10.5603/EP.a2018.0084.
[18] P. Schulz-Knappe, H.D. Zucht, G. Heine, M. Jürgens, R. Hess, M. Schrader, Peptidomics: the comprehensive analysis of peptides in complex biological mixtures, Comb. Chem. High Throughput Screen. 4 (2001) 207–217. https://doi:10.2174/1386207013331246.
[19] H. John, M. Walden, S. Schäfer, S. Genz, W.G. Forssmann, Analytical procedures for quantification of peptides in pharmaceutical research by liquid chromatography-mass spectrometry, Anal. Bioanal. Chem. 378 (2004) 883–897. https://doi:10.1007/s00216-003-2298-y.
[20] I. van den Broek, R.W. Sparidans, J.H. Schellens, J.H. Beijnen, Quantitative bioanalysis of peptides by liquid chromatography coupled to (tandem) mass spectrometry, J. Chromatogr. B 872 (2008) 1–22. https://doi:10.1016/j.jchromb.2008.07.021.
[21] M. Ewles, L. Goodwin, Bioanalytical approaches to analyzing peptides and proteins by LC-MS/MS, Bioanalysis 3 (2011) 1379–1397. https://doi:10.4155/bio.11.112.
[22] E. Machtejevas, H. John, K. Wagner, L. Ständker, G. Marko-Varga, W. G. Forssmann, R. Bischoff, K.K. Unger, Automated multi-dimensional liquid chromatography: sample preparation and identification of peptides from human blood filtrate, J Chromatogr B Analyt Technol Biomed Life Sci 803 (2004) 121–130. https://doi: 10.1016/j.jchromb.2003.07.015.
[23] D.C. Dallas, A. Guerrero, E.A. Parker, et al., Current peptidomics: applications, purification, identification, quantification, and functional analysis, Proteomics 15 (2015) 1026–1038. https://doi:10.1002/pmic.201400310.
[24] H.R. Sobhi, B. Vatansever, A. Wortmann, E. Grouzmann, B. Rochat, Generic approach for the sensitive absolute quantification of large undigested peptides in plasma using a particular liquid chromatography-mass spectrometry setup, J. Chromatogr. A 1218 (2011) 8536–8543. https://doi:10.1016/j.chroma.2011.09.072.
[25] Y.Q. Xia, M. Jemal, Phospholipids in liquid chromatography/mass spectrometry bioanalysis: comparison of three tandem mass spectrometric techniques for monitoring plasma phospholipids, the effect of mobile phase composition on phospholipids elution and the association of phospholipids with matrix effects, Rapid Commun. Mass Spectrom. 14 (2009) 2125–2138. https://doi: 10.1002/rcm.4121.
[26] A. Pezeshki, V. Vergote, S. Van Dorpe, et al., Adsorption of peptides at the sample drying step: influence of solvent evaporation technique, vial material and solution additive, J. Pharmaceut. Biomed. Anal. 49 (2009) 607–612. https://doi:10.1016/j.jpba.2008.12.003.
[27] K.D. Speicher, O. Kolbas, S. Harper, D.W. Speicher, Systematic analysis of peptide recoveries from in-gel digestions for protein identifications in proteome studies, J. Biomol. Tech. 11 (2000) 74–86.
[28] M. Goebel-Stengel, A. Stengel, Y. Taché, J.R. Reeve Jr., The importance of using the optimal plasticware and glassware in studies involving peptides, Anal. Biochem. 414 (2011) 38–46. https://doi:10.1016/j.ab.2011.02.009.
[29] K.L. Zapadka, F.J. Becher, A.L. Gomes Dos Santos, S.E. Jackson, Factors affecting the physical stability (aggregation) of peptide therapeutics, Interface Focus 7 (2017) 20170030. https://doi:10.1098/rsfs.2017.0030.
[30] R. Qiu, J. Xiao, X. Dong Chen, Multi-peptide adsorption on uncharged solid surfaces: a coarse-grained simulation study, Engineering 6 (2020) 186–195, https://doi.org/10.1016/j.eng.2018.12.012.
[31] P. Teuffel, M. Goebel-Stengel, T. Hofmann, et al., A RAPID method for blood processing to increase the yield of plasma peptide levels in human blood, J Vis Exp 110 (2016) 53959. https://doi:10.3791/53959.
[32] F. Alarcón, M. Díaz, F. Moyano, et al., Characterization and functional properties of digestive proteases in two sparids; gilthead seabream (Sparus aurata) and common dentex (Dentex dentex), Fish Physiol. Biochem. 19 (1998) 257–267, https://doi.org/10.1023/A:1007717708491.
[33] E.H. Lee, J.E. Park, J.W. Park, J.S. Lee, Purification and biochemical characterization of a fibrin(ogen)olytic metalloprotease from Macrovipera mauritanica snake venom which induces vascular permeability, Int. J. Mol. Med. 34 (2014) 1180–1190. https://doi:10.3892/ijmm.2014.1864.
[34] Z. Wu, G. Jiang, P. Xiang, D. Yang, N. Wang, Purification and characterization of trypsin-like enzymes from North Pacific krill (Euphausia pacifica), Biotechnol. Lett. 30 (2008) 67–72. https://doi:10.1007/s10529-007-9511-6.

[35] A.L. Huston, B. Methe, J.W. Deming, Purification, characterization, and sequencing of an extracellular cold-active aminopeptidase produced by marine psychrophile Colwellia psychrerythraea strain 34H, Appl. Environ. Microbiol. 70 (2004) 3321–3328. https://doi:10.1128/AEM.70.6.3321-3328.2004.
[36] R. Inzitari, T. Cabras, D.V. Rossetti, et al., Detection in human saliva of different statherin and P-B fragments and derivatives, Proteomics 6 (2006) 6370–6379. https://doi:10.1002/pmic.200600395.
[37] E.J. Helmerhorst, G. Traboulsi, E. Salih, F.G. Oppenheim, Mass spectrometric identification of key proteolytic cleavage sites in statherin affecting mineral homeostasis and bacterial binding domains, J. Proteome Res. 9 (2010) 5413–5421. https://doi:10.1021/pr100653r.
[38] M.S. Lamkin, F.G. Oppenheim, Structural features of salivary function, Crit. Rev. Oral Biol. Med. 4 (1993) 251–259. https://doi:10.1177/10454411930040030101.
[39] W.L. Siqueira, F.G. Oppenheim, Small molecular weight proteins/peptides present in the in vivo formed human acquired enamel pellicle, Arch. Oral Biol. 54 (2009) 437–444. https://doi:10.1016/j.archoralbio.2009.01.011.
[40] A.M. Lynge Pedersen, D. Belstrøm, The role of natural salivary defences in maintaining a healthy oral microbiota, J. Dent. 80 (Suppl 1) (2019) S3–S12. https://doi:10.1016/j.jdent.2018.08.010.
[41] G. Goobes, R. Goobes, O. Schueler-Furman, D. Baker, P.S. Stayton, G.P. Drobny, Folding of the C-terminal bacterial binding domain in statherin upon adsorption onto hydroxyapatite crystals, Proc. Natl. Acad. Sci. U.S.A. 103 (2006) 16083–16088. https://doi:10.1073/pnas.0607193103.
[42] F. Trindade, F. Amado, J. Pinto da Costa, et al., Salivary peptidomic as a tool to disclose new potential antimicrobial peptides, J. Proteomics 115 (2015) 49–57. https://doi:10.1016/j.jprot.2014.12.004.
[43] L.P. Morin, Neuroanatomy of the extended circadian rhythm system, Exp. Neurol. 243 (2013) 4–20. https://doi:10.1016/j.expneurol.2012.06.026.
[44] T.C. Gent, C.A.R. BassettI, Adamantidis. Sleep-wake control and the thalamus, Curr. Opin. Neurobiol. 52 (2018) 188–197. https://doi:10.1016/j.conb.2018.08.002.
[45] J.D. Miller, Cardiovascular calcification: orbicular origins, Nat. Mater. 12 (2013) 476–478. https://doi:10.1038/nmat3663.
[46] F. Domínguez, V. Fuster, J.M. Fernández-Alvira, et al., Association of sleep duration and quality with subclinical atherosclerosis, J. Am. Coll. Cardiol. 73 (2019) 134–144. https://doi:10.1016/j.jacc.2018.10.060.
[47] C.S. McAlpine, M.G. Kiss, S. Rattik, et al., Sleep modulates haematopoiesis and protects against atherosclerosis, Nature 566 (2019) 383–387. https://doi:10.1038/s41586-019-0948-2.
[48] H.M. Ochs-Balcom, K.M. Hovey, C. Andrews, et al., Short sleep is associated with low bone mineral density and osteoporosis in the women's health initiative, J. Bone Miner. Res. 35 (2020) 261–268. https://doi:10.1002/jbmr.3879.
[49] C.M. Swanson, W.M. Kohrt, P. Wolfe, et al., Rapid suppression of bone formation marker in response to sleep restriction and circadian disruption in men, Osteoporos. Int. 30 (2019) 2485–2493. https://doi:10.1007/s00198-019-05135-y.
[50] M. Markiewicz, E. Richard, N. Marks, A. Ludwicka-Bradley, Impact of endothelial microparticles on coagulation, inflammation, and angiogenesis in age-related vascular diseases, J. Aging Res. 2013 (2013) 734509. https://doi:10.1155/2013/734509.
[51] Y. Liu, C.M. Shanahan, Signalling pathways and vascular calcification, Front. Biosci. 16 (2011) 1302–1314. https://doi:10.2741/3790.
[52] K. Fijorek, M. Püsküllüoğlu, D. Tomaszewska, R. Tomaszewski, A. Glinka, S. Polak, Serum potassium, sodium and calcium levels in healthy individuals - literature review and data analysis, Folia Med. Cracov. 54 (2014) 53–70.
[53] T. Saito, The vascular clock system generates the intrinsic circadian rhythm of vascular contractility, J. Smooth Muscle Res. 51 (2015) 95–106. https://doi:10.1540/jsmr.51.95.